

321107
P. 31

(NASA-CR-184231) HIGH TEMPERATURE MATERIALS
CHARACTERIZATION Final Report (Alabama
Univ.) 31 p

N92-10079

CSSL 11F

Unclass

G3/26 0321107

Final Report

submitted to

NATIONAL AERONAUTICS AND SPACE ADMINISTRATION
GEORGE C. MARSHALL SPACE FLIGHT CENTER, ALABAMA 35812

December 31, 1990

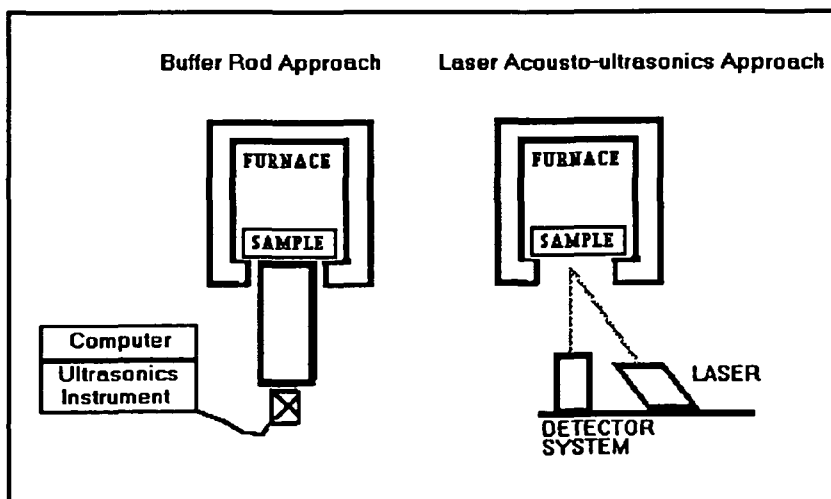
for NAS8 -36955 D.O. 47

entitled

High Temperature Materials Characterization

by

Gary L. Workman, PhD.
Principal Investigator



Johnson Research Center
The University of Alabama in Huntsville
Huntsville, Alabama 35899

TABLE OF CONTENTS

1.0	INTRODUCTION	1
2.0	COMPUTATIONS	5
3.0	EXPERIMENTAL RESULTS	7
4.0	CONCLUSIONS	21
5.0	ACKNOWLEDGEMENTS	21
6.0	BIBLIOGRAPHY	22
	APPENDIX A. THEORETICAL CONCEPTS	24
	APPENDIX B. PROCEDURES	27

1.0 INTRODUCTION

1.1 RESEARCH OBJECTIVES

This primary objective of this research was to determine the feasibility of a laboratory capability to determine elastic constants of materials from room temperature up to 1500 - 2000 ° F. The resulting project can then be divided into two sub-tasks. During the first phase of the task, a furnace assembly for the determination of elastic constants using ultrasonic velocity measurements was fabricated. After construction of the furnace assembly, the second phase of the project was used to perform experiments using the Matec MB8000 system in order to optimize upon various methods of coupling ultrasonic signals into the specimens at these elevated temperatures. In addition one set of experiments was run using a laser ultrasonics system to determine the feasibility of that technique.

This research has pointed out the significance of this measurement technique in the determination of materials characteristics which would be difficult to obtain otherwise and also re-emphasized the difficulties that still reside with the implementation of the technique, particularly if the desire is to set up a routine measurement capability. As demonstrated in this work, the individuals performing the measurements do have to develop considerable expertise with the technique and the Matec instrumentation in order to perform the measurements reliably throughout the temperature range of the furnace.

1.2 ULTRASONIC VELOCITY MEASUREMENTS FOR THE DETERMINATION OF MATERIALS CHARACTERISTICS

Stress and strain in materials can be expressed most simply in terms of Hooke's law. That is, the structure of the material can be described by atoms held together by springs and most simply, the strain is directly proportional to the stress. Hooke's law applies to small strains to avoid plastic deformation. A more in-depth discussion of the theory underlying this work is presented in Appendix A.

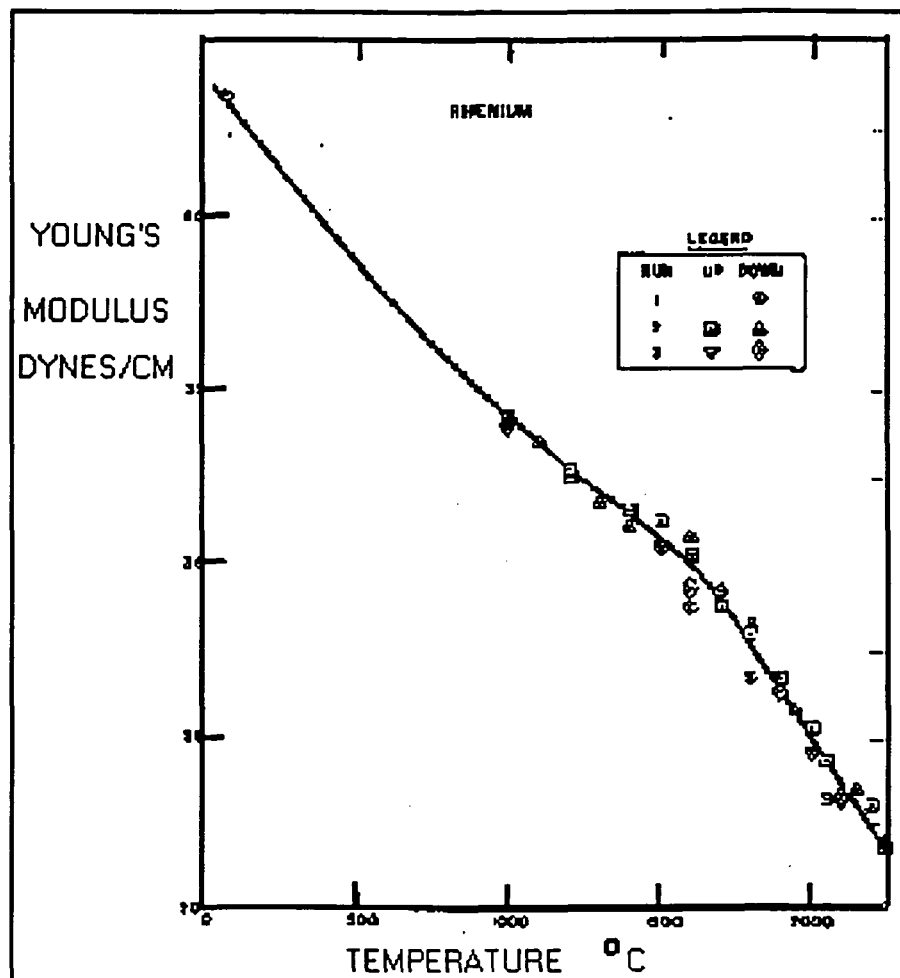
A considerable amount of materials information can be obtained about the crystalline properties of a material by determining the elastic constants over the desired temperature range¹. It is interesting to note that a traditional nondestructive testing technique such as ultrasonics can provide information about phase transformations, dislocations in single crystals, and even radiation effects in single crystal materials². This technique can then serve as a complementary measurement to assist in determining the usefulness of a material for service at high temperatures, . Materials in service in such hostile environments can then be monitored for change in structure once characteristic elastic constants are determined.

There is some information in the literature which reports on the types of materials characterization which can be obtained through the use of elastic constant determination. Most experimental work is quite tedious and has been reserved to academic research and some nuclear materials research activities. There certainly seem to be some gaps in the types of materials studied. For example, we have not found any major effort in determining elastic constants of materials such as superalloys to be reported in the literature. That is not to say that aerospace companies may have performed some research in the area, but have only published internal documentation on their results.

References 1 and 2 do contain a lot of information about the studies that had been performed up to the time of their submission for publication. Since no standardization in techniques or procedures had formalized up to that time, the techniques discussed were in general quite different from the technique used with either the Matec System or the laser system presented here.

The usefulness of using changes in elastic constants to determine a particular materials property is quite evident. For instance Figure 1 shows how a phase transformation in Rhenium at 1700 ° C was found. This approach developed in response to the need to monitor materials exposed to radiation at high temperatures in nuclear reactors.

Figure 1. Elastic constants of Rhenium from room temperature to the melting point.



1.2 HISTORICAL DEVELOPMENT

The theoretical and experimental development of elasticity has seen constant progress for many years. Early work in theoretical computations was fostered in the quantum physics community in the 1930 - 1950 era when much of the noted quantum mechanics work prospered. For example much of the foundation for numerical computation in elastic properties occurred in the work of Max Born and his associates in trying to predict materials properties from absolute zero all the way up the melting point^{3,4}. Since the atomic potentials of the structure are required for *a priori* computation

of the elastic forces, it makes sense that quantum physicists would be the group of scientists interested in that research.

Experimental work at that time was primarily centered around static measurements of elastic constants^{2,5}. Primarily the experiments measured volume changes on pure materials in known crystallographic orientations under stress. Since the major goals of that time period were to develop methods to compute and measure properties of materials, they worked primarily with single crystals and other simple structures. Scientific objectives dominated the desire to predict from first principles the properties of materials and only simple crystalline materials could be investigated with the computing power available. Engineering or metallurgical applications were considered too complex at that time. The static methods give elastic constants which are isothermal and can differ slightly from values obtained from the dynamic measurements such as the ultrasonic techniques⁴. The precision of static measurements also was limited by the ability to measure small strains. X-ray diffraction techniques still provide a useful tool for that measurement.

The early work using ultrasonic techniques focused on resonance frequency experiments and at a later time began to measure the time of flight of low frequency elastic waves through materials at room temperature^{2,4,5}. As faster electronic systems evolved, the ability to measure time-of-flights in microseconds allowed non-resonance techniques to become useful. The desire to go to higher frequencies was accomplished only by using multiple echoes and pulse echo overlap techniques with oscilloscope displays, such as the ring-around technique¹. Further improvement in electronics allowed the ability to measure time of flight of higher frequency elastic waves by more direct methods^{1,8}. The references listed above not only describe the measurement techniques developed during their respective time periods, but also provide a good indication of the accuracy and precision of the various techniques.

The ultrasonic techniques, for both resonance and time-of-flight measurements, provides adiabatic constants since the stress wave passes through the crystal volume, vibrating the atoms without transferring thermal excitation to the crystal. This can be compared with the older static measurement techniques, as described above.

2.0 COMPUTATIONS

Ultrasonics is useful for this type of measurement in that the velocities of ultrasonic waves depend strictly upon the elastic properties of materials. Hence the following relations, derivable from Hooke's Law, are used to calculate adiabatic elastic constants from velocity measurements. Appendix A contains a more in-depth description of the effects of the crystalline structure on the interpretation of elastic moduli and subsequently how one would interpret ultrasonic velocity measurements along various crystallographic axes.

Note that in the normal relations defined for shear modulus, G and Young's modulus, E are given as:

$$(1) \quad G = v_s^2 \rho \quad \text{and} \quad E = v_l^2 \rho$$

This relation for E holds only for slender rods. For bulk materials one uses the definition of the bulk modulus B , which is defined by

$$(2) \quad B = \frac{E}{3(1-\nu)} \quad \text{where } \nu \text{ is Poisson's ratio.}$$

Thus for non-slender materials, which is more characteristic of our samples, one uses

$$(3) \quad E = v_l^2 \rho \frac{(1+\nu)(1-2\nu)}{(1-\nu)}$$

to calculate Young's modulus. Likewise, G can be calculated from E using:

$$(4) \quad G = \frac{E}{2(1+\nu)}.$$

For the laser generation of surface waves the most useful way to obtain G from a surface wave velocity is to use

$$(6) \quad G = c_T^2 \rho / 0.895.^9$$

Then the relations given above are used to determine E and B, knowing Poisson's ratio.

The variation of elastic constants with temperature is normally expressed through the use of the Duhamel-Neumann equation:

$$(7) \quad \sigma_{ij} = \lambda \delta_{ij} \epsilon_{kk} + 2 \mu \epsilon_{ij} - \alpha (3 \lambda + 2 \mu)(T - T_0) \delta_{ij}$$

where α is the thermal expansion of the material and the other variables are defined in Appendix A. Note that the temperature variation is a function of the change in volume due to thermal expansion of the material.

Another useful set of relations which we found to be useful in evaluating the use of buffer rods for the determination of elastic constants are the definition of the acoustic impedance, given by $Z = v_l \rho$ and definitions of reflection coefficient and transmission coefficient. Thus

$$(8) \quad R = \frac{(Z_2 - Z_1)}{(Z_2 + Z_1)} \quad \text{and} \quad T = \frac{2Z_2}{(Z_2 + Z_1)}$$

or if $r = \frac{Z_2}{Z_1}$ the one can use the alternate formulation for R and T; i.e.

$$(9) \quad R = \frac{r - 1}{r + 1} \quad \text{and} \quad T = \frac{2r}{(r + 1)}$$

The importance of these equations will be seen in section 3 since they affect how one needs to interpret the experimental data. These relations ultimately determine the ability to launch acoustic waves into specimens and discriminate the appropriate signals for determining the positioning of gates for use with the Matec instrumentation.

3.0 EXPERIMENTAL RESULTS

3.1 HIGH TEMPERATURE FURNACE SYSTEM

The ultrasonic measurement system developed in this work uses a Model 3320 Split Tube furnace from Applied Test Systems, Inc.. The split tube furnace was chosen in order to simplify sample exchange when performing experiments. The inside dimensions of the furnace determine the sample sizes allowed. The model purchased for this work has an inside diameter of 2 inches and a heated length of 10 inches. Maximum temperature for this furnace is rated at 1700 °C or 2668 °F when maximum power of 2940 watts is used.

Temperature control is provided by a Eurotherm model 818 temperature controller using a model 462 SCR power controller assembly. A type S thermocouple provides the sensing required for the temperature control. We have used these temperature controllers in several of our KC-135 flight furnaces used for microgravity materials processing experiments and have been very pleased with their performance.

3.2 ULTRASONIC VELOCITY MEASUREMENTS

3.2.1 TECHNIQUES USED IN THIS STUDY

The two techniques that were studied for this project were a.) the use of a quartz buffer rod to couple the acoustic energy to the specimen and b.) a pulsed laser diode source of acoustic energy. The quartz buffer rod and its many variations have been used for many years while pulsed lasers are relatively new. Figure 3. shows conceptually how

the two techniques relate to each other. In section 3.4 some comparisons between the current capabilities of each technique will be given.

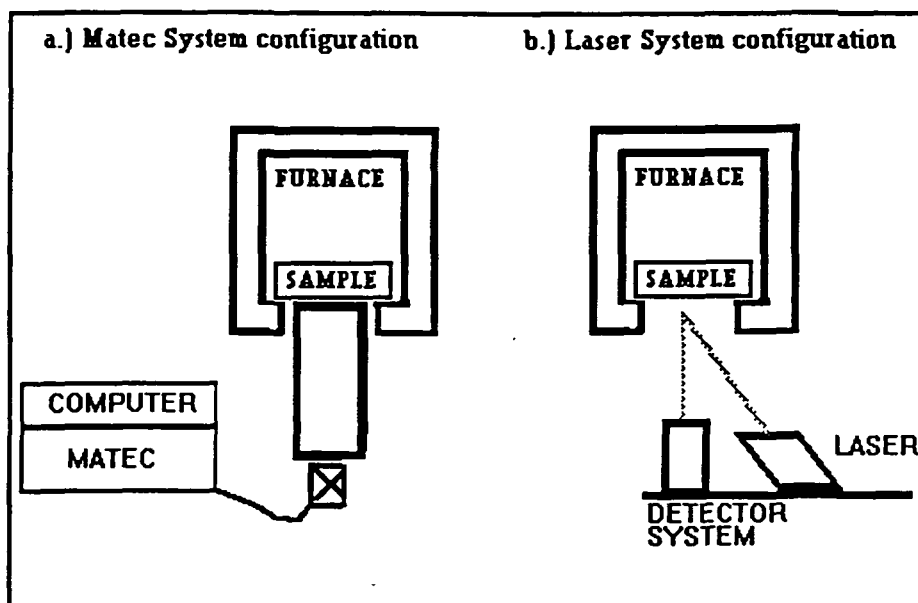


Figure 2. Experimental configurations for the quartz buffer rod technique and the pulsed laser system.

3.2.1 QUARTZ BUFFER RODS

As mentioned in the introduction, the availability of electronic circuits which could measure time-of-flight of rf bursts of acoustic energy in the nanosecond regime opened up a new capability for elastic constant determination. Many researchers have participated in making such measurements, particularly at room temperature. The number of measurements at high temperatures is less numerous due to the difficulties required in making such measurements.

The published literature presents some of the potential sources of error in measuring time of flight using buffer rods:^{1,8,9}

1. Mode converted signals from sidewall reflections.
2. Dispersion

3. Transducer and sample bond (acoustic coupling)
4. Phase Cancellation
5. Wave Diffraction.

Mode conversion is handled in either of two ways: 1) by calculating the divergence of the acoustic beam at the frequency of interest and then use a buffer rod larger than the divergence of the beam or 2) to use a thin waveguide (or wire) assuming that only one mode will be able to propagate through the waveguide. We chose to use the former concept and implemented a 1" diameter quartz buffer rod.

Acoustic energy losses at the interfaces during the travel of the ultrasonic beam play an important part in determining the travel time of the beam. Generally an oscilloscope display has to be used to determine the proper time sequences at which the primary ultrasonic pulse occurs and the occurrences of the various reflected signals from the interfaces in the ultrasonic propagation system. In this case the ultrasonic propagation system consists of both the sample and the buffer rod. In order to differentiate among the possible reflected pulses from each interface, an estimate of the travel time is made and one then looks for a pulse within that time frame. For instance the ultrasonic velocity of an aluminum sample will always lie around 6.3×10^3 meters/second, decreasing with temperature, as shown in equation 7. The exact value will then be determined from the measurement process. In order to select the proper reflected signals for the measurement, one must know from the oscilloscope display, which signals to set the gate. Figure 3, shown on the next page, illustrates how an idealized ultrasonic velocity measurement system would be configured in a pulse echo arrangement. It is important to note that the two interfaces labelled in the schematic play an important role in making measurements with the system. The effect of the coupling between the two materials at each interface will always deteriorate the signal amplitudes one is trying to measure. Consequently a major effort has been made to optimize the transmission characteristics of the coupling agents in the experiments performed in this work.

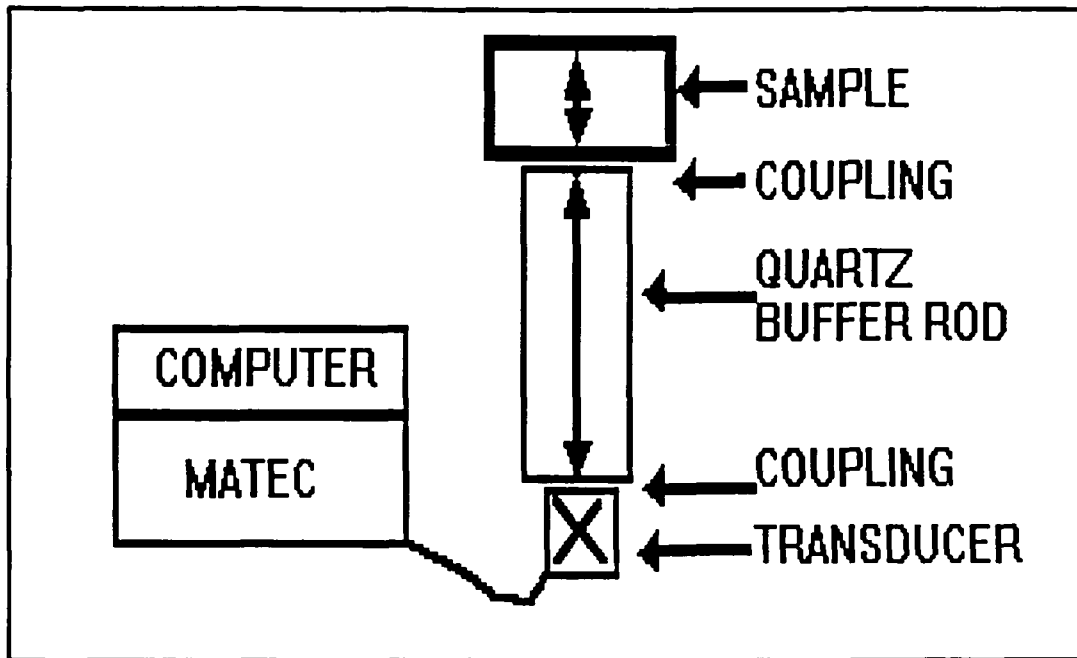


Figure 3. Typical system configuration used to measure ultrasonic velocities with a buffer rod.

The Matec System B8000 provides a technique which does not depend upon ultrasonic signal amplitudes as much as previous instrumentation. Using phase-sensitive measurement procedures, the intent of the technique is to measure phase changes in the desired ultrasonic signals and avoid spurious amplitude variations due to coupling problems or phase cancellation effects such as observed by destructive interference effects in the many ultrasonic beams which might propagate in the measurement system. This effect is described in more detail in the next paragraph. It is useful to remember that the use of phase-sensitive methods for the determination of ultrasonic velocity measurements is characteristic of the Matec approach.

For the purposes of better understanding how the Matec system works, it is important to understand the significance of phase cancellation. The ultrasonic signals used in this work were longitudinal waves, which means that the acoustic pressure of the measurement pulse is a superposition of the waves being received at the transducer. If two reflected pulses traveling two different paths, happen arrive at the receiving

transducer at the same time, then out-of-phase superposition of the pressure waves can result in observation of a reduced signal amplitude due to destructive interference. Hence it can occur that one may not even see the reflected wave from the surface of interest.

Phase relationships can also affect the precision of the time-of-flight measurements^{1,6,7,8}. Since the transmitted pulse is a sinusoidal wave train, there is no precise point (or amplitude) from which to measure in determining the actual travel time of the acoustic energy. At each reflecting interface small phase changes occur in the amplitude of the reflected energy with respect to the transmitted energy. The overall effect is to produce an uncertainty in the actual travel time of the ultrasonic energy. The discussion of the phase sensitive method used by the Matec system will illustrate this phenomenon.

3.3 MATEC SYSTEM OPERATION

3.3.1 THEORY OF OPERATION

The Matec MBS - 8000 Ultrasonic Test System uses a phase sensitive measurement technique to measure the time of flight. Earlier techniques based on matching a particular point on a wave amplitude display have serious sources of errors. The Matec system was designed to by-pass some these sources of error.

The method used by the Matec system compensates for discrepancies in amplitude and signals with contributing phase effects is to use a phase-locked loop concept as shown in Figure 4 on the next page.

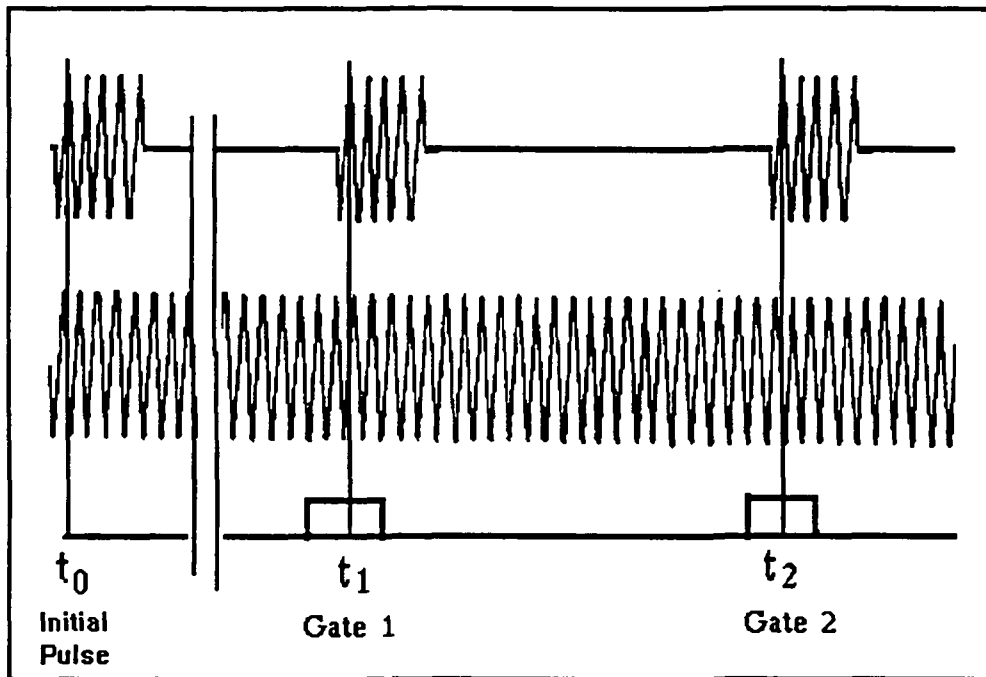


Figure 4. Waveforms used in Matec MBS-8000 System for velocity measurements.

The two upper waveforms, labelled Gate 1 and Gate 2, represent reflections from the front and back surfaces of the sample respectively. As described in the previous commentary, it is difficult to precisely measure from a specific waveform position, such as the first maximum amplitude, in each of these wave-forms. However if a continuous sinusoidal waveform is used as a reference waveform (or time-scale) throughout the ultrasonic transmission and reception process, then one has a ruler with which to compare with at all times. Then the phase detector will measure the proper time for the waveform position, with respect to the reference waveform, not from a reflected waveform which may be distorted. The proper expression for the time of flight then becomes:

$$\Delta t = \frac{\Delta \phi}{2\pi f}$$

where $\Delta \phi$ is the phase change between output pulse and received waveform. The software supplied from Matec performs the task of making this measurement for the user.

3.3.2 LABORATORY OBSERVATIONS

The Matec MBS -8000 System, which had been purchased previously by MSFC for materials characterization purposes, was set up and used in this study. Both students working with the system spent considerable time and effort in learning how to use the system optimally. The instructions provided by the manufacturer were not easily converted into day-to-day use of the system. For that reason we have included a discussion about the trial and error procedures developed during this contract and Appendix 2 as a compilation of procedures which were implemented in order to get consistency in the measurement process. Even at that, good data is difficult to get, especially at higher temperatures.

For example a typical oscilloscope display for setting gates to make measurements looks like Figure 5.

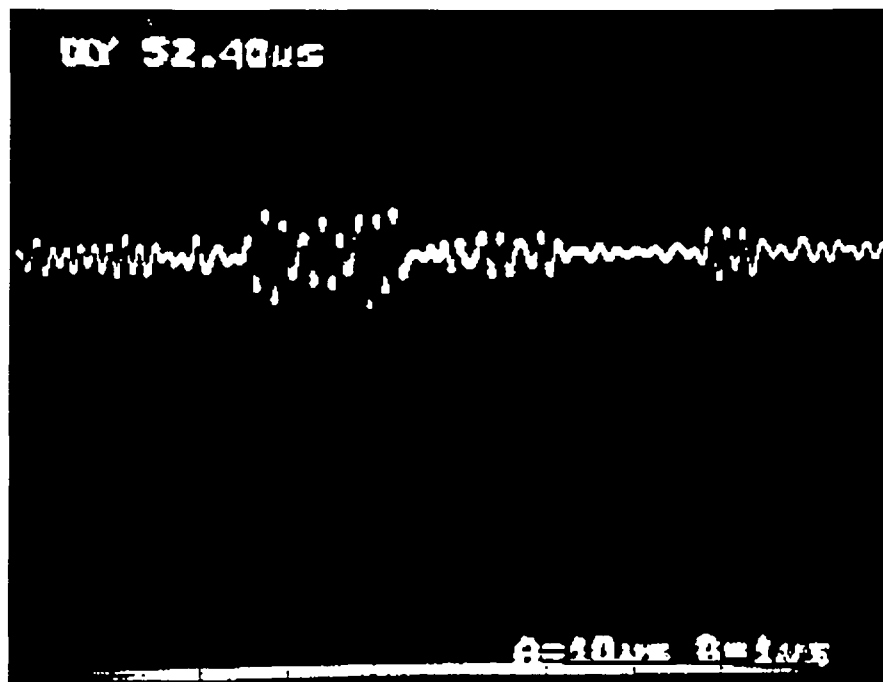


Figure 5. Oscilloscope display showing types of waveforms observed by detector probe.

Operational procedures issued by the manufacturer stressed the importance of setting the ultrasonic gates at several reflections from the specimen walls. Most of time, particularly with the buffer rod measurements, the oscilloscope displays were extremely difficult to use in order to discern the appropriate reflected waveforms. Choosing echos by sight on the oscilloscope screen was not completely accurate. Many echoes would overlap due to propagation through each material set (transducer, buffer rod and sample). Prior knowledge of the anticipated travel time was required most of the time in order to set the gates on the the correct signals.

The students modified the Basic program supplied by Matec to also include the capability to print out velocity values and standard deviations for each sets of readings. Standard deviation in the measurements taken varied from 0.020 μ seconds to as high as 0.5 μ seconds in the normal measurement mode using the 10 measurement averaging algorithm. Reproducibility of test results was always a problem.

Sonotrace couplant was the best interface couplant tried in this study, but it did not allow for very high temperature range. However it was always used for the coupling material between the ultrasonic transducer and the buffer rod. That interface does not normally go above ambient temperature. Several other coupling agents were tested for the high temperature interface, but none were really successful. Teflon tape^{10,11} had been reported in two journal articles, however our attempts with it gave poor results. Molten metals have also been suggested¹², however, we feel that alloying of the specimen might give erroneous results also.

Best results for the higher temperatures were epoxy materials obtained from Aremco Ceramics. This company offers several blends of adhesives for bonding metals to ceramics. Several procedures were developed to obtain useful bonding with these materials. Generally these adhesives worked well at high temperatures until the ceramic baked dry. At this point the acoustic bonds impaired echo transmissions to a point that

not enough energy could get through the various interfaces in order to averaging of more than two echoes.

Even with good bonding, the reflections assigned to the sample interfaces will decrease with temperature because of the variation of the reflection coefficient with acoustic impedance (equations 8 or 9). Note that as the temperature of the sample increases, the density ρ of the sample decreases and the reflection coefficient decreases linearly with respect to temperature. The thermal coefficient for quartz is assumed to be negligible relative to the aluminum sample. Calculations of these two phenomena are shown in Figures 5 and 6 which follow.

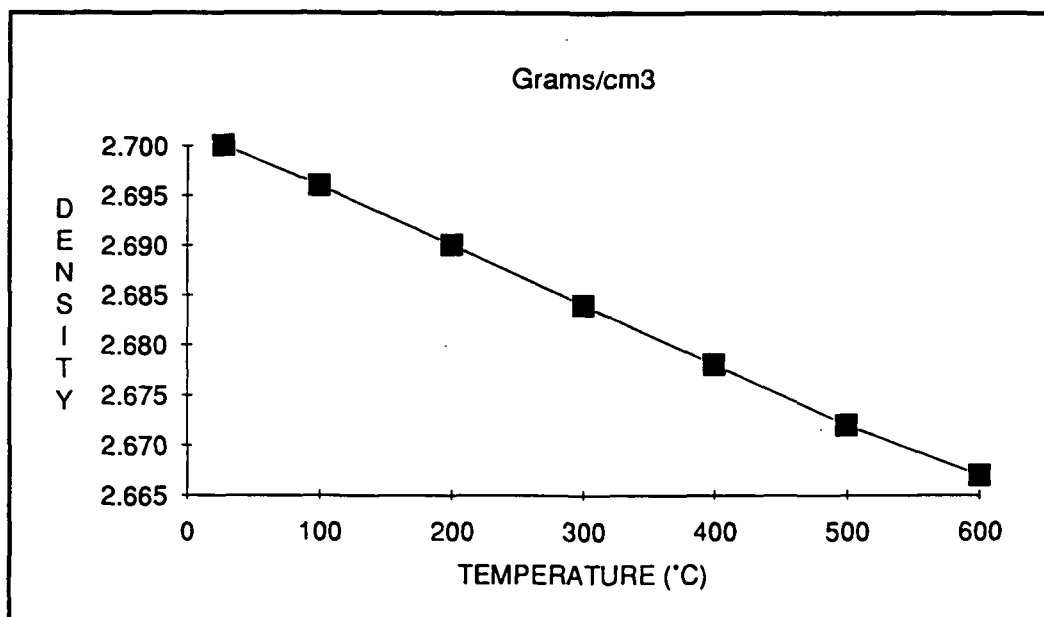


Figure 5. Calculated density change for aluminum with temperature.

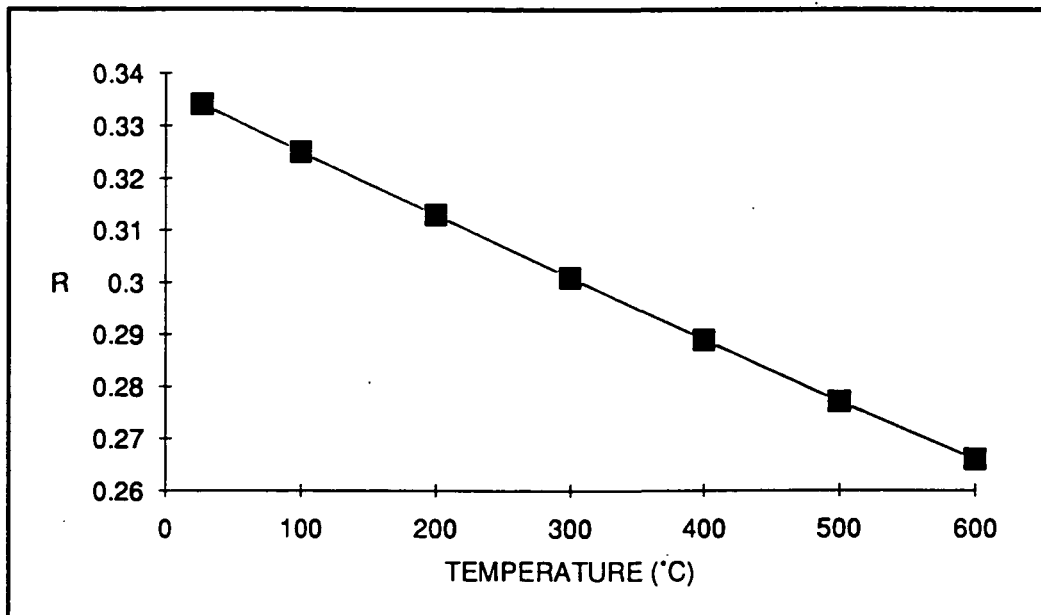


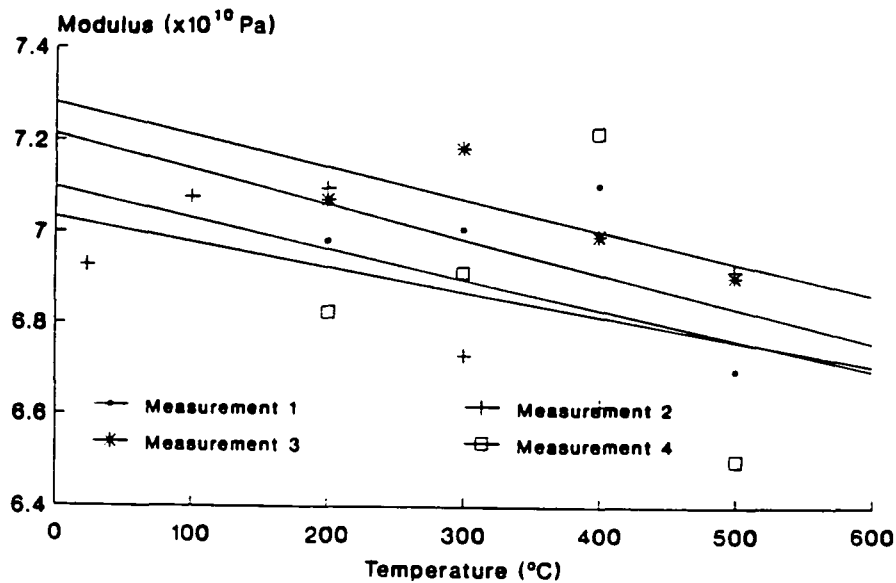
Figure 6. Calculated reflection coefficient for Al-SiO₂ interface which shows how decreasing reflection coefficient with increasing temperature. This helped to explain increased difficulty with the high temperature measurements.

The students made a number of observations on experimental results obtained with the Matec system. For instance, the Matec manual says that optimal measurement technique is to position the gate just past the midpoint of the echo peak. We never observed that this position gave any better results than any other. Usually the highest point in the peak was used. This seemed to give the best results. Usually the smallest gate width was used for marking echoes.

The pulser amplitude, as displayed on the adjustments menu, was not adjustable above 446 millivolts, . A larger amplitude capability would have been able to transmit the energy through the various interfaces and allowed for better discrimination of the smaller echoes. Recently new literature from Matec indicates that higher power systems are available. It appears that this problem will not occur in future systems.

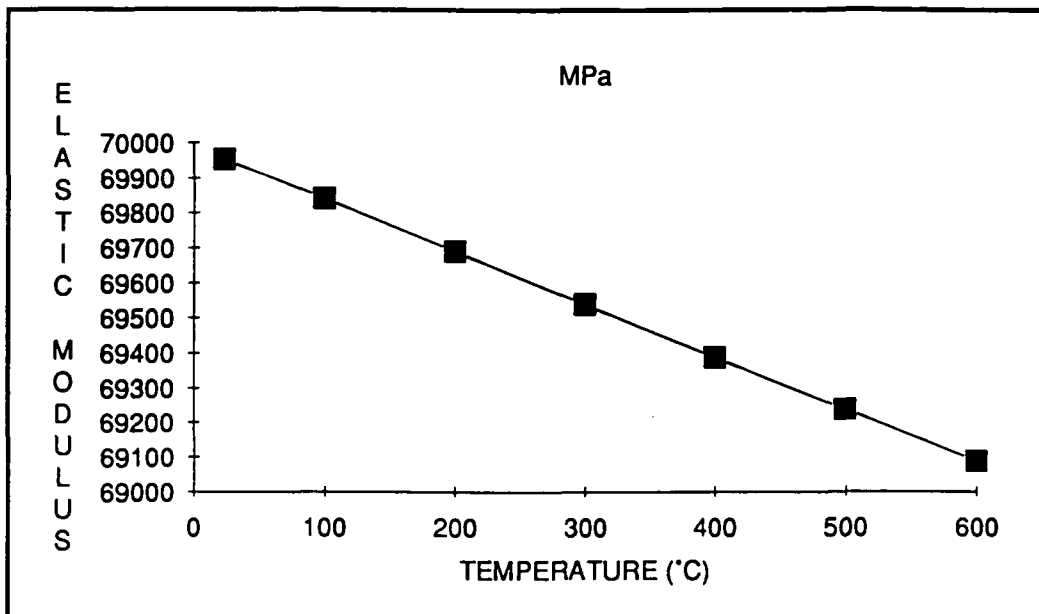
The data collected from a temperature excursions to 500 °C gives calculated bulk modulus using equation (3) is given in Figure 7. This graph shows a lot of scatter in the data.

Figure 7. Measured Bulk Modulus of Aluminum



Note that the data does follow a linear variation in E with respect to temperature as predicted from the Duhamel-Neuman thermoelastic equation. A simple equation relating the change in E to the coefficient of expansion changes with temperature for aluminum is given in Figure 8.

Figure 8. Calculated Bulk Modulus of Aluminum.



3.4. LASER ACOUSTO-ULTRASONICS MEASUREMENT

The NDE Laboratory at the Johns Hopkins¹³ University, under Dr. Robert E. Green Jr., have built an laser generated and measurement system for determining elastic constants for the NASA/Lewis Research Center. We were able to sub-contract a visit from the graduate student doing the work to travel to Huntsville and perform a measurement for us using the M&P Laboratory furnace. Mr. Robert Huber was able to come to Huntsville in August and spent two days working with Mr. Bill Smith on the tests.

The laser system has a lot of merit for this type of measurement in that data is fairly easy to obtain from reflective surfaces. The experimental arrangement was shown in Figure 2. The student, Robert Huber, had very few problems in setting up the instrument with the M&P furnace assembly and then to take data. Alignment procedures seemed to be fairly straight-forward. The focal length of the system was pre-set and had

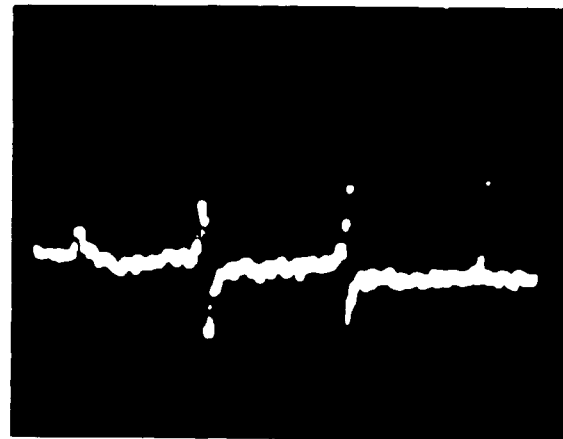
sufficient room to set up the system. As mentioned previously this particular system was to be delivered to Lewis Research Center upon completion of their grant period.

The laser generated acoustic wave which was observable with the interferometric system was a Rayleigh wave traveling along the surface of the specimen. Hence the measured elastic constants are representative of only the materials at the surface of the specimen and not within the bulk. Hence the elastic constant calculated from this quantity is G , the shear modulus.

Figure 9. shows the waveform obtained from the laser acousto-ultrasonic measurement. The value of G obtained from that measurement is given by equation 6 or

$$G = v_r^2 \rho / 0.895 = 25.1 \times 10^9 \text{ Pascals.}$$

Figure 9. Laser acousto-ultrasonic waveform which gives $v_r = 2.89 \times 10^3 \text{ m/sec.}$



| 16.5mm |

t_0 t_1

5.7 microseconds

The precision of the technique is still quite poor as the students were not able observe variation in the elastic constant measurement from 23 to 250 ° C. This is due to the lack of either accuracy or precision in interpreting oscilloscope displays for the measurement.

The literature quotes a corresponding value of 27.5 Pascals for Aluminum alloys¹⁶. We do not know what alloy our specimen was, hence there is no need to try and determine any error in results from the technique. We can then calculate $E = 33.6 \times 10^9$ Pascals and $B = 67.6 \times 10^9$ Pascals . The literature quotes 72.4×10^9 Pascals for B¹⁶. Note that at 23 °C using the quartz buffer rod, we obtained an elastic modulus of 69×10^9 Pascals.

3.5 ACCOMPLISHMENTS AND RECOMMENDATIONS

- a) Fabrication of delivery of high temperature furnace.
- b) Experimental verification of elastic constant determination with Matec system.
- c.) Experimental verification of elastic constant determination with laser system.
- d) Evaluation of several types of materials for high temperature coupling.

Recommendations include:

- a) Continue research into coupling agents for high temperatures. Several other materials have been suggested since contract terminated. This technique will be useful for characterizing high temperature components. A mor structured sample set would be useful in that regard.
- b) Increase ultrasonic transducer energy to obtain stronger reflected signal as noted above. Even Matec provides the capabilities now.
- c) Further research into the capabilities of the laser ultrasonics system. If the precision and accuracy are improved, the technique will be quite useful in high temperature materials programs.

4.0 CONCLUSIONS

A laboratory facility for measuring elastic moduli up to 1700 ° C has been constructed and delivered to Marshall Space Flight Center. We have demonstrated that the ultrasonic method can be used to determine elastic constants of materials from room temperature to their melting points. The ease in coupling high frequency acoustic energy is still a difficult task and needs further refinement. Even as the report was being written new coupling materials and higher power ultrasonic pulsers have been suggested to us. The current work was only able to scratch the surface in terms of showing the full capabilities of either technique used here, especially since there is such a large learning curve in developing proper methodologies to take measurements into the high temperature region. The laser acoustic system does not seem to have sufficient precision at this time to replace the normal buffer rod methodology.

A recommendation which can be made is to continue the work with a more structured set of samples in order to improve and verify the precision of the measurement techniques. It is also worthwhile to consider developing the laser ultrasonic technique at Marshall Space Flight Center. The types of samples of interest to Marshall Space Flight Center are probably different from those of interest to Lewis Research Center. M & P Laboratory may want to consider having its own capability in that area. The costs are not high, time and effort to assemble the system and obtain expertise are the major costs.

5.0 ACKNOWLEDGEMENTS

The assistance of the students, Bill Smith and Jeffrey Haight in performing the many tasks required for construction of the furnace assembly and running the tests is very much appreciated. The helpfulness of Robert Bond, for finding the right parts when needed, is also appreciated. Also appreciation is owed to Mr. Tom Morris of M&P Laboratory for his assistance as TCOR on the contract.

5.0 BIBLIOGRAPHY

1. Papadakis, E. P., **Ultrasonic Velocity and Attenuation: Measurement Methods with Scientific and Industrial Applications**, *Physical Acoustics XII*, Academic Press, New York, 1976 pp 227 -374.
2. Huntington, H. B., **The Elastic Constants of Crystals**, *Solid State Physics 7* (1958) pp 213 - 351.
3. Born, M., *Jour. Chem Phys.* 7 (1939) 591 - 603.
4. Hearmon, F. R. S., **The Elastic Constants of Anisotropic Materials**, *Phys. Rev.* (1956) pp 323 - 382
5. Kittel, **Solid State Physics**, pp. 111 - 129, John Wiley and Sons, New York, 1967
6. McSkimmin, H. J., **Pulse Superposition Method for Measuring Ultrasonic Wave Velocities in Solids**, *Jour. Acous. Soc.*, 33 (1961) pp 12-16.
7. McSkimmin, H. J., **Notes and Comments for the Measurement of Elastic Moduli by Means of Ultrasonic Waves**, *Jour. Acous. Soc.*, 33 (1961) pp 606 - 615.
8. Breazeale, M. A., J. H. Cantrell Jr., and J. S. Heyman, **Ultrasonic Wave Velocity and Attenuation Measurements**, appearing in *Methods of Experimental Physics vol. 19, Ultrasonics*, Academic Press, New York, 1981, ed. Edmonds, P. D.
9. Lynnworth, L. C., **Ultrasonic Measurements for Process Control**, Academic Press, Boston, 1989.
10. Drescher-Krasicka, E., J. N. Meder, and A. V. Granato, **A Teflon pressure-transducer-specimen bond for ultrasonic measurements over a wide temperature range**, *Int J. of NDT*
11. Drescher-Krasicka, E., **An Ultrasonic Sensor for Process Modelling and Process Control of Ceramic Superconductors**, QNDE to be published.
12. Mahmoud, M. A., **Low Melting Alloys used as Ultrasonic Couplants at High Temperatures**, *Mat. Eval.* 43, (1985) pp. 196 - 200.
13. Huber, R. D. and R. E. Green Jr., **Acousto-ultrasonic Nondestructive Evaluation of Materials Using Laser Beam Generation and Detection**,

presented at the *Second Conference on Nondestructive Evaluation for Aerospace Requirements*, 1989 , Huntsville

14. Silk, M. G. , **Ultrasonic Transducers for Nondestructive Testing**, Adam Hilger, Bristol 1984.
15. Whitney, J. M., **Structural Analysis of Laminated Anisotropic Plates**, Technomic Publishing Company, Lancaster, PA 1987.
16. Dieter, G. M., **Mechanical Metallurgy**, McGraw Hill, New York 1986.
17. Breazeale, M. A. and Jacob Philip, **Determination of Third Order Elastic Constants from Ultrasonic Harmonic Generation Measurements**, *Physical Acoustics XVII*, Academic Press, New York, 1984 pp 2 -57.
18. Ensminger, D., **Ultrasonics**, Marcel Dekker, New York, 1973
19. Aussel, J. D. and J. P. Monachalin, **Precision laser-ultrasonic velocity measurement and elastic constant determination**, *Ultrasonics* 27 (1987) pp 165 - 177.
20. Piche, L., B. Champagne, and J. P. Monachalin, **Laser Ultrasonics Measurement of Elastic Constants of Composites**, *Mat. Eval.* 45, (1987) pp. 74 - 79.
21. Mehrabian, R. and H. N. G. Wadley, **Needs for Process Control in Advanced Processing of Materials**, *Progress in Quantitative Nondestructive Evaluation*
22. Thompson, R. B., **Relative Anisotropies of plane waves and guided waves in thin orthorhombic plates; implications for texture characterization**, *Ultrasonics* 26 (1988) pp 133 - 138.
23. Aussel, J. D., A. L Le Brun and J. C. Baboux, **Generating acoustic waves by laser: theoretical and experimental study of the emission source**, *Ultrasonics* 26 (1988) pp 245 - 255.
24. Birch, F., **Finite Elastic Strain of Cubic Crystals**, *Phys. Rev.* 71 (1947) pp 809 - 824.
25. Thurston, R. N. **Third-Order Elastic Constants and the Velocity of Small Amplitude Elastic Waves in Homogenously Stressed Media**, *Phys. Rev.* 133 (1964) pp A1604 - 1610.
26. Graff, K. F., **Wave Motion in Elastic Solids**, Ohio University Press, Columbus, 1975

27. Abramov, O. V. , O. M. Gradov, and M. I. Yudin, **Non-linear effects of acoustic generation in solids**, *Ultrasonics* 28 (1990) pp 83 - 89.
28. Cielo, P., F. Nadeau, and M. Lamontagne, **Laser generation of convergent acoustic waves for materials inspection**, *Ultrasonics* 24 (1985) pp 55 - 62.

APPENDIX A. THEORETICAL CONCEPTS

An excellent discussion on mechanical metallurgy and the various approaches currently used to classify materials and their engineering properties is given in Reference 16. Classical laws of physics can then be used to macroscopically define the elasticity properties of the materials. The structure of the material defines the number of constants required to adequately describe the elasticity properties of the material. For instance Figure A-1. illustrates a cubic material with vectors indicating directional forces on the structure. The strains resulting from these forces define the elastic constants.

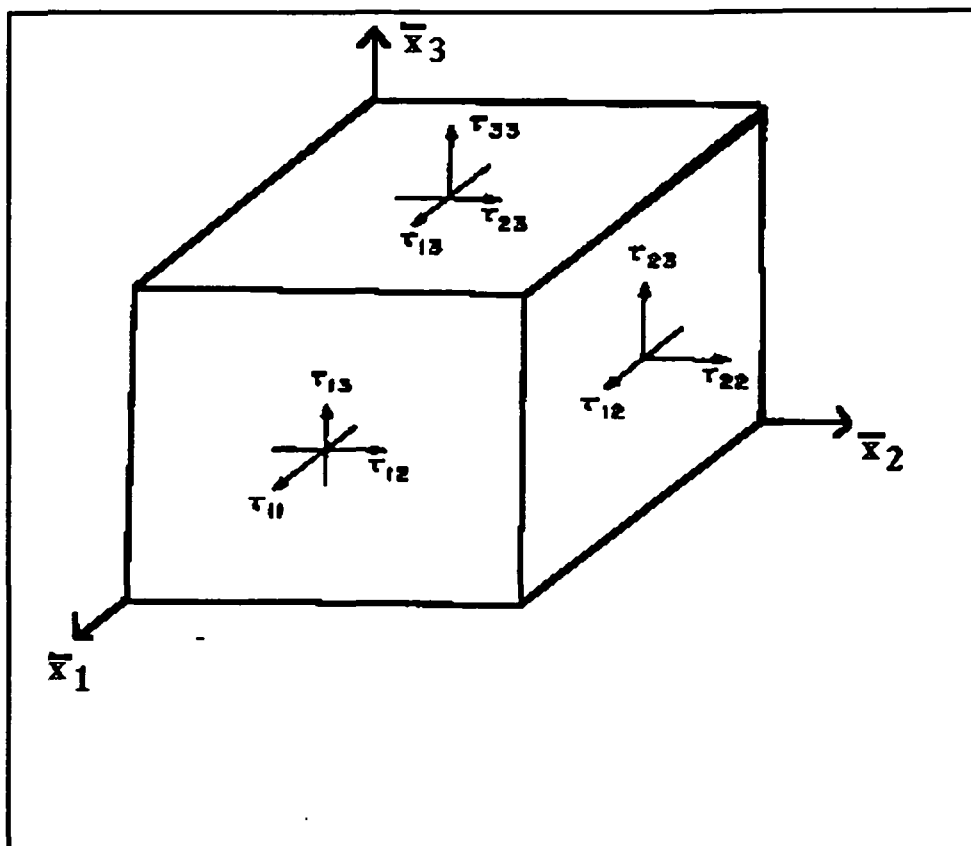


Figure A-1. Unit cell of cubic material showing stress and strain components of force vectors.

For the general case there are 21 independent elastic constants, such that stress = (stiffness matrix) X strain or:

$$\begin{pmatrix} \sigma_{11} \\ \sigma_{22} \\ \sigma_{33} \\ \sigma_{23} \\ \sigma_{13} \\ \sigma_{12} \end{pmatrix} = \begin{pmatrix} c_{11} & c_{12} & c_{13} & c_{14} & c_{15} & c_{16} \\ c_{12} & c_{22} & c_{23} & c_{24} & c_{25} & c_{26} \\ c_{13} & c_{23} & c_{33} & c_{34} & c_{35} & c_{36} \\ c_{14} & c_{24} & c_{34} & c_{44} & c_{45} & c_{46} \\ c_{15} & c_{25} & c_{35} & c_{45} & c_{55} & c_{56} \\ c_{16} & c_{26} & c_{36} & c_{46} & c_{56} & c_{66} \end{pmatrix} \begin{pmatrix} \epsilon_{11} \\ \epsilon_{22} \\ \epsilon_{33} \\ \epsilon_{23} \\ \epsilon_{13} \\ \epsilon_{12} \end{pmatrix}$$

If there is one plane of symmetry, say the x_3 axis is perpendicular to a plane of symmetry then:

$$c_{14} = c_{15} = c_{24} = c_{25} = c_{34} = c_{35} = c_{46} = c_{56} = 0$$

and the number of independent elastic constants reduces to 13. The stiffness matrix then becomes:

$$\begin{pmatrix} \sigma_{11} \\ \sigma_{22} \\ \sigma_{33} \\ \sigma_{23} \\ \sigma_{13} \\ \sigma_{12} \end{pmatrix} = \begin{pmatrix} c_{11} & c_{12} & c_{13} & 0 & 0 & c_{16} \\ c_{12} & c_{22} & c_{23} & 0 & 0 & c_{26} \\ c_{13} & c_{23} & c_{33} & 0 & 0 & c_{36} \\ 0 & 0 & 0 & c_{44} & c_{45} & 0 \\ 0 & 0 & 0 & c_{45} & c_{55} & 0 \\ c_{16} & c_{26} & c_{36} & 0 & 0 & c_{66} \end{pmatrix} \begin{pmatrix} \epsilon_{11} \\ \epsilon_{22} \\ \epsilon_{33} \\ \epsilon_{23} \\ \epsilon_{13} \\ \epsilon_{12} \end{pmatrix}$$

Likewise if there are two mutually perpendicular planes of elastic symmetry, then we can also write $c_{33} = c_{22}$, $c_{13} = c_{12}$, $c_{55} = c_{66}$, and $c_{44} = \frac{c_{22} \cdot c_{23}}{2}$.

The number of independent elastic constants is now reduced to 5. The Hooke's law formulation now becomes:

$$\begin{pmatrix} \sigma_{11} \\ \sigma_{22} \\ \sigma_{33} \\ \sigma_{23} \\ \sigma_{13} \\ \sigma_{12} \end{pmatrix} = \begin{pmatrix} c_{11} & c_{12} & c_{12} & 0 & 0 & 0 \\ c_{12} & c_{22} & c_{23} & 0 & 0 & 0 \\ c_{12} & c_{23} & c_{22} & 0 & 0 & 0 \\ 0 & 0 & 0 & \frac{c_{22}-c_{23}}{2} & 0 & 0 \\ 0 & 0 & 0 & 0 & c_{66} & 0 \\ 0 & 0 & 0 & 0 & 0 & c_{66} \end{pmatrix} \begin{pmatrix} \epsilon_{11} \\ \epsilon_{22} \\ \epsilon_{33} \\ \epsilon_{23} \\ \epsilon_{13} \\ \epsilon_{12} \end{pmatrix}$$

For complete isotropy, the number of independent constants is reduced to 2 and the stiffness matrix now becomes:

$$\begin{pmatrix} \sigma_{11} \\ \sigma_{22} \\ \sigma_{33} \\ \sigma_{23} \\ \sigma_{13} \\ \sigma_{12} \end{pmatrix} = \begin{pmatrix} c_{11} & c_{12} & c_{12} & 0 & 0 & 0 \\ c_{12} & c_{11} & c_{12} & 0 & 0 & 0 \\ c_{12} & c_{12} & c_{11} & 0 & 0 & 0 \\ 0 & 0 & 0 & \frac{c_{11}-c_{12}}{2} & 0 & 0 \\ 0 & 0 & 0 & 0 & \frac{c_{11}-c_{12}}{2} & 0 \\ 0 & 0 & 0 & 0 & 0 & \frac{c_{11}-c_{12}}{2} \end{pmatrix} \begin{pmatrix} \epsilon_{11} \\ \epsilon_{22} \\ \epsilon_{33} \\ 2\epsilon_{23} \\ 2\epsilon_{13} \\ 2\epsilon_{12} \end{pmatrix}$$

where c_{11} is equivalent to the Lamé constant λ and $\frac{c_{11}-c_{12}}{2}$ is equivalent to the Lamé constant μ . This formulation of Hooke's law can be expressed as:

$$\begin{pmatrix} \sigma_{11} \\ \sigma_{22} \\ \sigma_{33} \\ \sigma_{23} \\ \sigma_{13} \\ \sigma_{12} \end{pmatrix} = \begin{pmatrix} \lambda+2\mu & \lambda & \lambda & 0 & 0 & 0 \\ \lambda & \lambda+2\mu & \lambda & 0 & 0 & 0 \\ \lambda & \lambda & \lambda+2\mu & 0 & 0 & 0 \\ 0 & 0 & 0 & \mu & 0 & 0 \\ 0 & 0 & 0 & 0 & \mu & 0 \\ 0 & 0 & 0 & 0 & 0 & \mu \end{pmatrix} \begin{pmatrix} \epsilon_{11} \\ \epsilon_{22} \\ \epsilon_{33} \\ 2\epsilon_{23} \\ 2\epsilon_{13} \\ 2\epsilon_{12} \end{pmatrix}$$

Since aluminum in particular is a homogenous material, we are able to utilize the Lamé constants λ and μ for this work.

APPENDIX 2. PROCEDURE FOR ULTRASONIC MATERIALS CHARACTERIZATION WITH THE MATEC MBS 8000

1.0 Software Set-Up

1.1 Power on all components of the system.

1.2 Enter <BR835> in computer to execute batch file for Matec software. Main menu will appear.

1.3 Use function keys as shown on display to set parameters for test.

1.4 Typical settings on Aluminum sample are:

Repetition Rate - 10.0 milliseconds

Pulse Width - 0.25 microseconds

Gate width - between 0.1 and 0.5 microseconds

Receiver Gain - 0.0 dB

Frequency - 5.0 MHz

Amplitude - 0.445 V (Maximum allowed by software)

Filter Setting - #2

1.5 Toggle the printer on using the [+] key

1.6 In setting the gate positions for a measurement, it is recommended that at least three reflections be gated for an accurate measurement. It is recommended also that the gates be placed just past the highest peak of a reflection for best identification by the system.

2.0. Using the Hitachi V-660 Oscilloscope for Measurement

There is a large percentage of reflected echoes that appear on the screen. Some are possibly due to side wall reflections in the quartz buffer rod. Others are of

uncertain origin. In order to obtain the correct reflections on the screen, the positions of the echoes need to be calculated and echoes nearest these calculated areas are expected to be the correct echoes.

- 2.1 Connect the two inputs from the MBS-8000 to the oscilloscope as shown in the Matec manual.
- 2.2 Set the VERTICAL mode switch to DUAL to show both the reflection wave form and the gate positioning form.
- 2.3 Use the positioning knobs for each channel to place the waves in the best position for the user.
- 2.4 Use the horizontal mode features of the oscilloscope to expand the area of possible interest by setting the ALT switch to on. This will show a second enlarged portion of the wave form on the screen in addition to the previous form which may be moved horizontally using the VARIABLES control knob.
- 2.5 The SELECTOR toggle may be set to A/B SEP to separate the waves using the VARIABLES control knob for user clarity.
- 2.6 Use the SELECTOR toggle switch to set the scope into DELAY mode.
- 2.7 The TIME/DIV selector may now be used to enlarge a particular segment of the wave form while the original form is shown without change. The screen will show the total delay for the enlarged portion of the wave in the upper left corner of the screen.
- 3.0. Eurotherm Controller for Heating the Furnace
- 3.1 Open the door at the bottom of the controller to show programming set controls.
- 3.2 Hold the right button until the SP1 read-out is shown.
- 3.3 Set the desired temperature for test with the UP and DOWN arrow buttons.
- 3.4 Close door. Readout will return to normal and furnace will begin heating.
- 3.5 After test the temperature may be changed to another desired temperature or to zero for cooling.